

UNCLASSIFIED

(NASA-CR-150208)	AVIATION SAFETY RESEARCH	N77-20047
AND TRANSPORTATION/HAZARD AVOIDANCE AND		
ELIMINATION Final Report (Raytheon Co.)		
54 p HC A04/MF A01	CSSL 01C	Unclas
		21725
	G3/03	

AVIATION SAFETY RESEARCH AND  
 TECHNOLOGY/HAZARD AVOIDANCE AND ELIMINATION  
 FINAL REPORT  
 NAS8-30795

ER76-4220

August 1976

Prepared for  
 GEORGE C. MARSHALL SPACE FLIGHT CENTER  
 NASA  
 Huntsville, Alabama 35812



**RAYTHEON COMPANY**  
 EQUIPMENT DIVISION



UNCLASSIFIED

RAYTHEON COMPANY

EQUIPMENT DIVISION

RAYTHEON

AVIATION SAFETY RESEARCH AND  
TECHNOLOGY/HAZARD AVOIDANCE AND ELIMINATION  
FINAL REPORT

ER76-4220

August 1976

CONTRACT NAS8-30795

Prepared for  
GEORGE C. MARSHALL SPACE FLIGHT CENTER  
NASA  
Huntsville, Alabama 35812

Prepared by  
C. Sonnenschein  
C. DiMarzio  
D. Clippinger  
D. Toomey

RAYTHEON COMPANY  
EQUIPMENT DEVELOPMENT LABORATORIES  
ADVANCED DEVELOPMENT LABORATORY  
ELECTRO-OPTICS DEPARTMENT  
Sudbury, Massachusetts 01776

## TABLE OF CONTENTS

<u>SECTION</u>		<u>PAGE</u>
1	INTRODUCTION	1-1
1.1	Introduction	1-1
1.2	Synopsis	1-3
1.2.1	Aircraft Wake Vortices	1-3
1.2.2	The Laser Doppler System	1-5
1.2.3	Dust Devils	1-14
1.2.4	Data Analysis	1-14
2	VORTEX TIME HISTORIES	2-1
2.1	Introduction	2-1
2.2	Data Processing Algorithm	2-1
2.3	Results	2-1
2.4	Transport Vs. Wind Comparison	2-3
2.5	Conclusions	2-9
3	EFFECTIVE CIRCULATION CALCULATIONS	3-1
3.1	Introduction	3-1
3.2	Methods of Calculation	3-1
3.3	Results	3-3
3.4	Conclusions	3-4
4	MULTIPLE VORTICES	4-1
4.1	Introduction	4-1
4.2	Models	4-1
4.3	Experimental Results	4-3
4.3.1	Introduction	4-3
4.3.2	Spectra	4-4
4.3.3	Multiple Vortex Velocity Profiles	4-5
4.3.4	Potential Effects of Multiple Vortices on Vortex Time Histories	4-8



TABLE OF CONTENTS (Cont'd)

<u>SECTION</u>		<u>PAGE</u>
	4.4 Conclusions	4-10
5	SYSTEM PERFORMANCE	5-1
6	CONCLUSIONS	6-1

## LIST OF ILLUSTRATIONS

<u>FIGURE</u>		<u>PAGE</u>
1-1	Trailing Vortex Wake	1-4
1-2	Laser Doppler Velocimeter Transmission and Reception	1-7
1-3	Laser Doppler Velocity Measurement	1-8
1-4	Illustration of Optical Heterodyning	1-9
1-5	Laser System Configuration	1-11
1-6	SLDV Block Diagram	1-12
1-7	Overall Diagram of the SLDVS	1-13
1-8	Gila River Indian Reservation Test Site	1-15
1-9	Vortex Signal Spectrum (Untranslated)	1-16
2-1	Sample Vortex Transport	2-2
2-2	Sample Vortex Transport	2-4
2-3	Sample Vortex Transport	2-5
2-4	Parameter Time History	2-6
2-5	Parameter Time History	2-7
2-6	Vortex Transport - Wind Profile Comparison	2-10
3-1	Method of Selecting Points for Velocity Profiles	3-5
3-2	Effective Circulation Vs. Time for B-747 Vortices in a Category II Wind	3-6
4-1	Typical Vortex Spectra	4-6
4-2	Scale Drawing of SLDV Scan Pattern and a B-747 Wing	4-7

## SECTION 1

## INTRODUCTION

1.1 INTRODUCTION

Data collected by the Scanning Laser Doppler Velocimeter System (SLDVS) has been analyzed to determine the feasibility of the SLDVS for monitoring aircraft wake vortices in an airport environment. Additionally, some data collected on atmospheric vortices at a test site near Phoenix, Arizona has been analyzed. The test of this system began at Marshall Space Flight Center in Huntsville, Alabama in the Spring of 1974. After the tests at MSFC, there were two test periods at Kennedy International Airport in New York, in the Fall of 1974 and the Spring of 1975. The atmospheric vortex data was collected at the Gila River Indian Reservation, south of Phoenix, Arizona, in August of 1975.

Over 1600 landings were monitored at Kennedy International Airport and by the end of the test period 95% of the runs with large aircraft were producing usable results in real time. The transport was determined in real time and post-analysis using algorithms which performed centroids on the highest amplitude in the thresholded spectrum. Making use of other parameters of the spectrum, vortex flow fields were studied along with the time histories of peak velocities and amplitudes.

The post-analysis of the data was accomplished with a CDC-6700 computer using several programs developed for LDV data analysis. These programs were also used as diagnostic aids during the early tests of the system. In this way, the LDV data analysis program aided in locating problems, in developing the real time algorithm, and in processing the data for more detailed information than could be obtained in real time.

Additionally, a statistical analysis was performed on a sample of the real time data to determine the system performance as a function

of different aircraft and atmospheric parameters. It was determined that the real time algorithm was capable of measuring vortex centers to at least  $\pm 10$  feet. Other studies of the real time data were undertaken to verify the correctness of the spectral parameters used in the real time analysis and to determine optimum parameter selection for performance of the algorithm.

In the early part of the program, simulations were performed to determine the best algorithm and parameters as well as to study the practical limits to location accuracy.

Modifications were made to the data processing algorithm to adapt it to data from atmospheric vortices, such as dust devils, and data from the Gila River Indian Reservation test site was processed. This analysis showed not only that the system was successful in detecting and tracking dust devils and measuring their flow fields, but also that a frequency translator installed in the system could produce data showing the sense of the velocity, making the velocity field measurements easier to interpret.

The results of this program have been presented in three interim reports. The first interim report dated 16 December 1974 covers the testing at Marshall Space Flight Center and the early part of the Kennedy International Airport tests in the Fall of 1974.<sup>(1)</sup> The second interim report dated 3 November 1975 includes all of the work done during both test periods at Kennedy International Airport, including a statistical analysis of a selected portion of the data and a preliminary system redesign.<sup>(2)</sup> The third interim report, dated 8 March 1976, deals exclusively with the dust devil data.<sup>(3)</sup> After a short description of the system and the data processing methods, it consists of a data presentation of selected velocity and amplitude profiles along with dust devil transport, peak velocity and backscatter time histories and sample circulation calculations.

The remainder of Section 1 presents a synopsis of the program since its beginning including brief discussions of vortices and the

operation of the SLDV. The later sections describe the work performed since the last interim report. Section 2 shows typical vortex time histories, including horizontal and vertical transport, as well as time histories of peak velocities and amplitudes. Section 3 describes the results of the effective circulation calculation and shows a number of examples. The evidence of multiple vortices in the aircraft wake observed during this data analysis is summarized in Section 4. A summary of the system performance is included in Section 5.

## 1.2 SYNOPSIS

### 1.2.1 AIRCRAFT WAKE VORTICES

The simplest form of an aircraft wake consists of a pair of counterrotating vortices, as shown in Figure 1-1. One vortex is shed from each wing and, according to theory, the vortex centers are separated by  $\pi/4$  times the wingspan. The direction of rotation is that which produces a downward velocity component between the vortices. According to the theory of line vortices, in the absence of any wind or other influence, the transport of the vortex center is determined by the induced velocity of the remaining vortex. If the pair is close to the ground, the interaction becomes more complicated due to the boundary condition of zero vertical velocity component at the ground. This condition may be handled by the introduction of reflections of the two vortices about the ground. These reflections or images, under the ground, combined with the actual vortices, satisfy the boundary condition and provide a simple means of determining vortex transport. The transport velocity of each vortex center is the vector sum of the induced velocity from the remaining vortices. Finally, the effect of wind may be considered by adding the local wind vector to the induced velocities. The predicted transport for a vortex pair is, initially, descent and horizontal motion with the ambient wind. At lower altitudes, the descent rate is reduced and the vortices begin to separate, while the center of the pair continues to move with the wind. Finally,



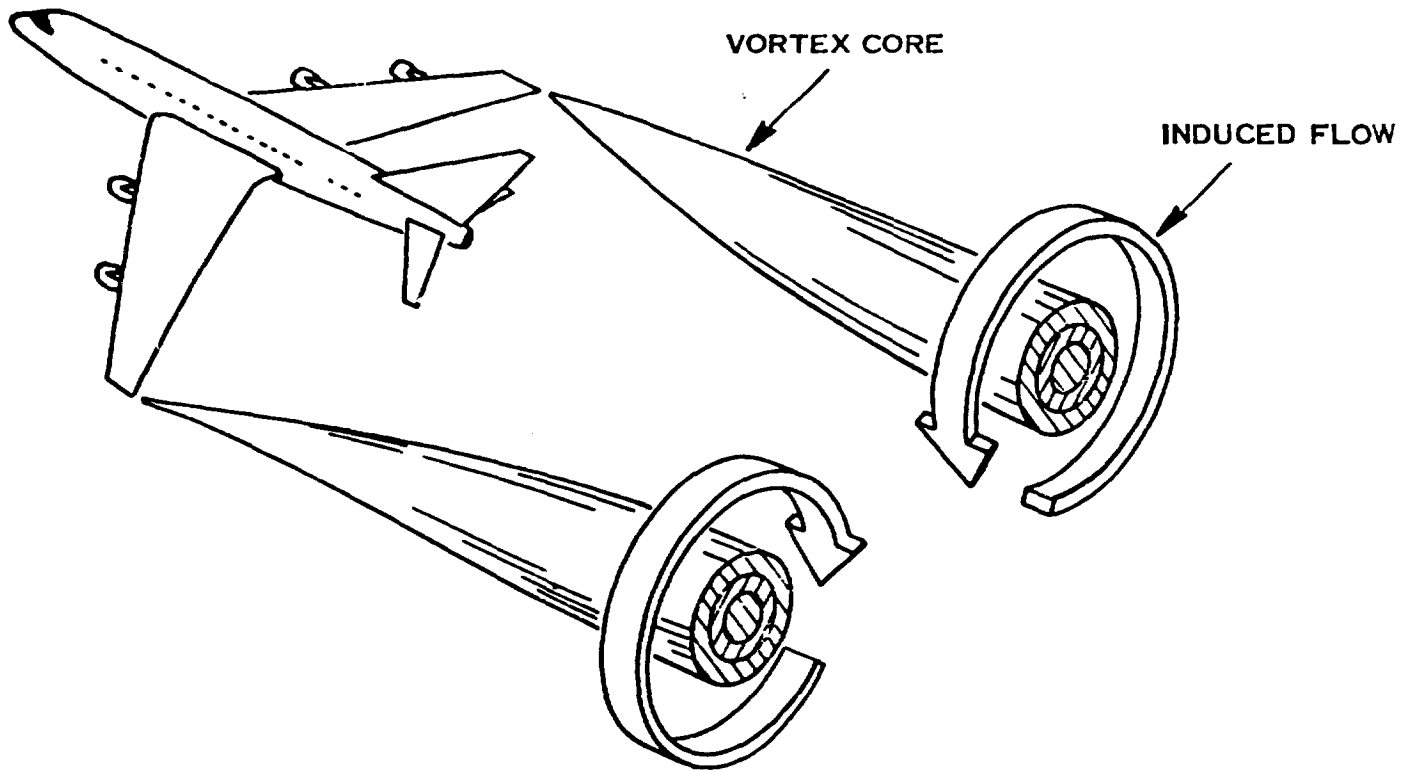


Figure 1-1. Trailing Vortex Wake.

the vortices are predicted to separate at a speed equal to twice the initial descent rate at a constant altitude of half the initial separation.

Thus, the aircraft wake presents a potentially hazardous situation to another aircraft encountering it. The situation is particularly severe on landing when aircraft are required to fly along the same flight path approaching the runway. The severity of the situation is determined by the size and weight of the generating and encountering aircraft and by meteorological conditions, including especially the ambient wind which influences transport and decay of the wake. The problem of wake vortices has thus led to separation requirements which decrease the capacity of larger airports. Since the transport and decay of vortices are influenced by many factors, separations are required at all times large enough to allow for the rare cases when the wake decays slowly and remain near the landing corridor. A vortex sensing system would permit measurements to be made to determine optimal separation standards as well as to determine the effectiveness of vortex abatement techniques.

### 1.2.2 THE LASER DOPPLER SYSTEM

The Scanning Laser Doppler Velocimeter (SLDV) is ideally suited for this application. It combines the excellent angular resolution of a focussed laser beam with the accurate velocity measurement ability of the Doppler technique. The SLDV measures the line-of-sight velocity component of aerosols naturally suspended in the atmosphere by determining the frequency shift of laser radiation backscattered from these aerosols. The vortex core, loosely defined as the cylinder on which the vortex velocity is a maximum, presents two regions of high line-of-sight velocity to a system scanning a plane perpendicular to the line along the center of the vortex. Vortex location may readily be accomplished by locating these areas.

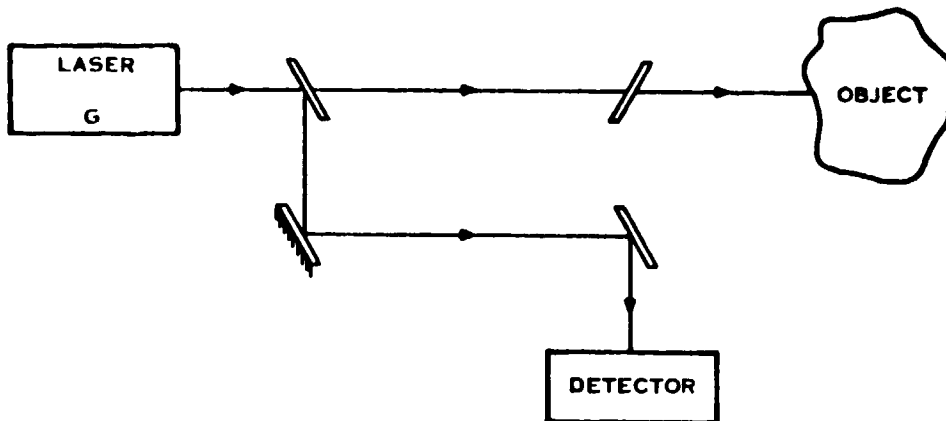
Operation of a laser Doppler velocimeter may be understood with the aid of Figure 1-2. A laser beam is transmitted through an interferometer which passes most of the energy to the target and diverts a small amount to the detector as shown in Figure 1-2a. The transmitted beam is usually passed through a telescope to the target which in the present case consists of naturally suspended aerosols in the atmosphere. Some of the transmitted energy is backscattered by the target particles and enters the detector by the path shown in Figure 1-2b. This returning energy has been shifted in frequency by an amount proportional to the component of particle velocity parallel to the direction of propagation according to the Doppler principle. Figure 1-3 shows the geometry of the laser system and target velocity vector relationship. Only the velocity component parallel to the propagation direction contributes to the Doppler shift.

Thus, there are two beams falling on the detector with two different frequencies as shown in Figure 1-4; a large reference beam at the optical frequency  $f_o$ , and the smaller signal beam at the new frequency  $f_o + f_d$  where  $f_d$  is the Doppler shift frequency. When these beams are added, the resulting beam contains a contribution at the difference of these frequencies.

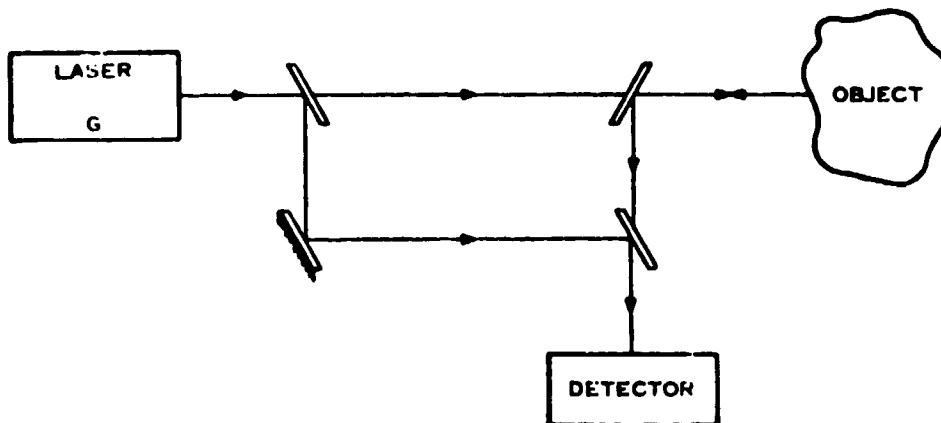
The difference, of course, is the Doppler frequency and may be related to the target velocity.

The power at each frequency is a measure of the product of the backscatter coefficient of the target particles which are moving at that frequency and the system response at that range and frequency. The system response is designed to be independent of frequency over large bandwidth. The response as a function of range may be controlled by focussing at a particular range so that the system response peaks sharply at that range.

The system used a stable  $CO_2$  laser beam expanded and focussed by a twelve-inch telescope. Range resolution was obtained by the focussing of the optical system. The range of focus was varied by movement of the telescope secondary and the elevation angle was



a) Paths of Transmitted Beam.



b) Paths of Transmitted and Received Beams.

Figure 1-2. Laser Doppler Velocimeter Transmission and Reception.

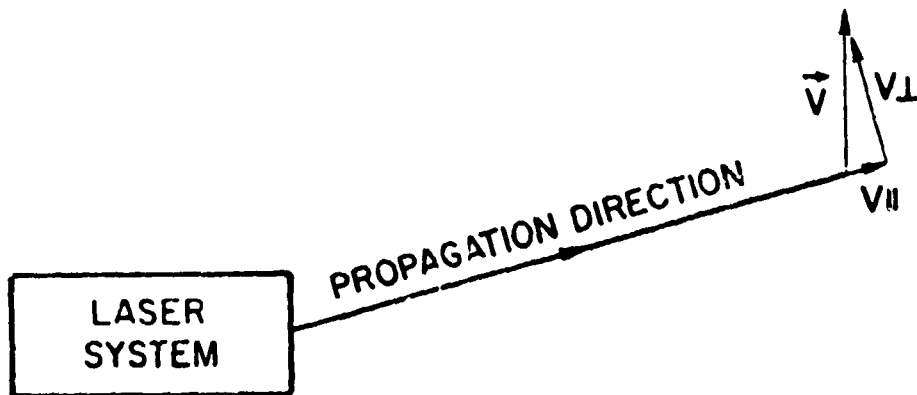


Figure 1-3. Laser Doppler Velocity Measurement.

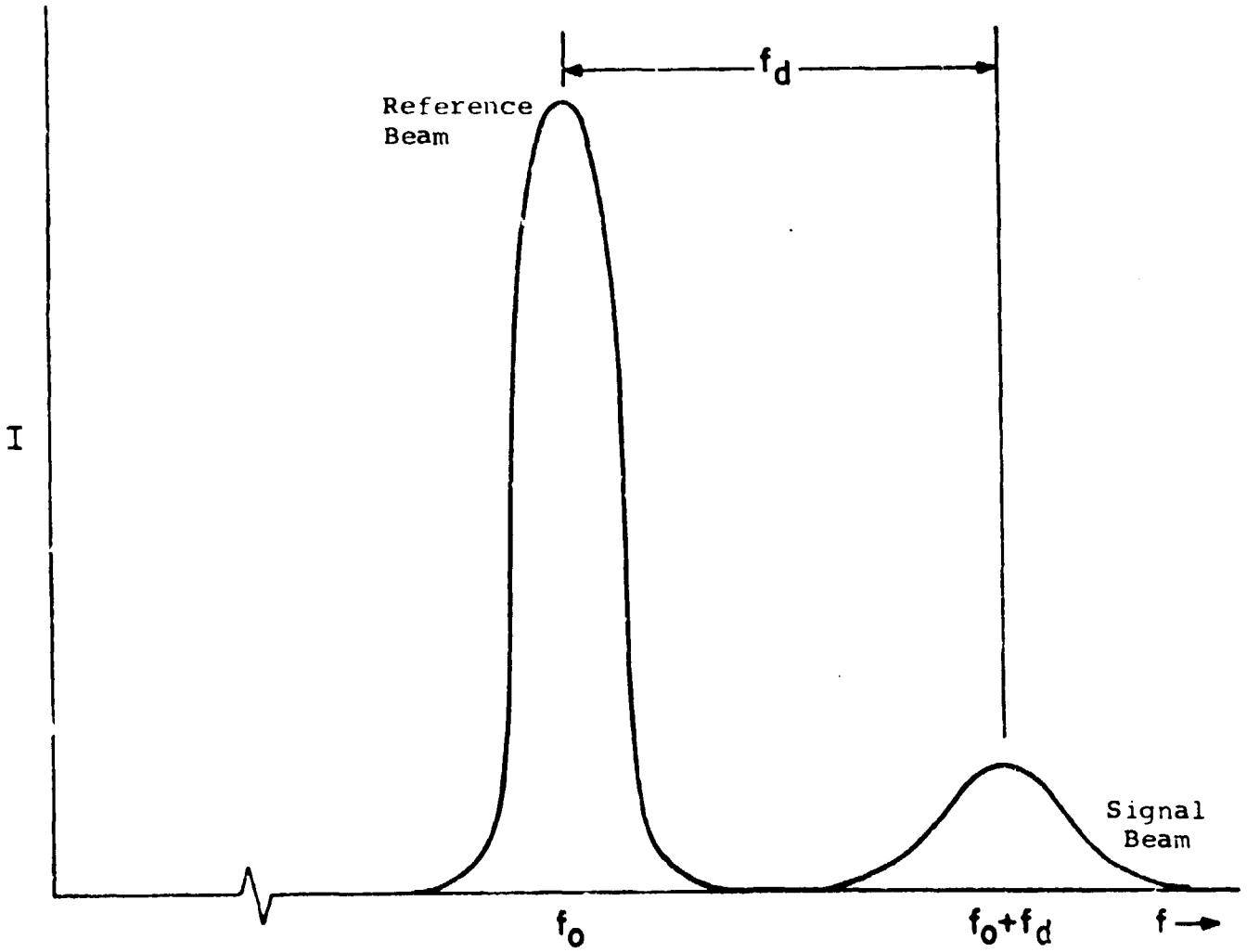


Figure 1-4. Illustration of Optical Heterodyning.

varied by means of a movable mirror reflecting the transmitted beam. By executing a fast range scan and a slow angle scan, the system scanned a vertical plane as shown in Figure 1-5. A spectral analysis of the heterodyne signal indicated the velocity of each volume of air. The processor thresholded the data, determining significant parameters of the spectrum and output them to the computer. The raw data, giving a complete description of the spectrum, was recorded in pulse code modulation (PCM) format on a high speed tape for later, more detailed analysis.

A block diagram of the system is shown in Figure 1-6. Laser radiation is separated by the interferometer into a reference or local oscillator (LO) beam of a few milliwatts and a transmitted beam of more than 10 watts. Optionally, a frequency translator is used to offset the LO frequency. The transmitted beam is passed through a telescope and scanning mirror to the target, reflected back through the telescope and superimposed on the LO in the interferometer. The combined signal is incident on an Hg:Cd:Te detector cooled to liquid nitrogen temperature (77K). The resulting electronic signal is processed by the signal processor to produce spectrum outputs to a high speed tape recorder and thresholded data to a minicomputer for real time analysis. The data presented in this report is from the high speed tapes.

An overall diagram of the SLDVS is shown in Figure 1-7. The system is mounted in an instrument van which is rigidly supported on a platform on the ground. The optical system is in the rear of the van with processing electronics, display and tape recorder in the middle, and computer in the front. The upper right corner of the figure shows a simple output. The X and Y coordinates are shown as functions of time on separate graphs. Additional outputs are available including Y as a function of X, tabular data, and diagnostic outputs. Furthermore, tape recordings are made of the complete spectrum every integration time for more detailed analysis.

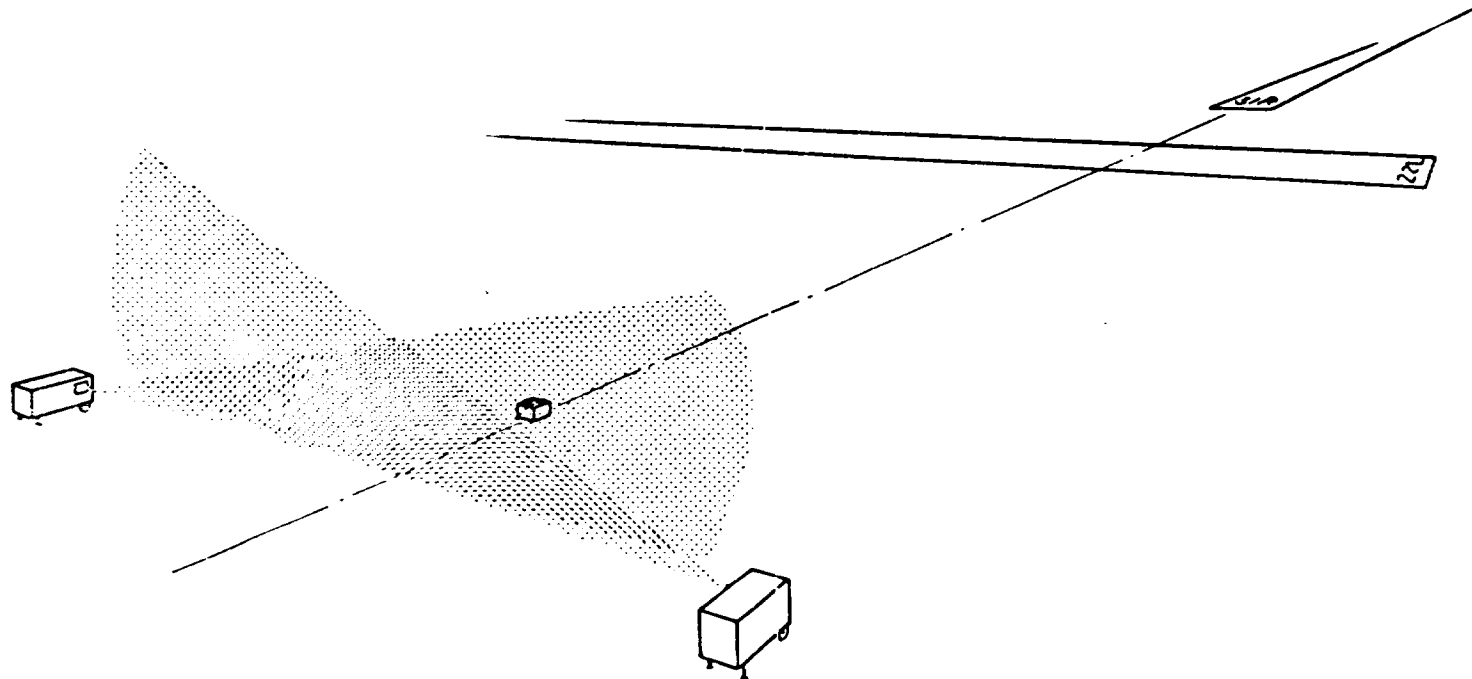


Figure 1-5. Laser System Configuration.



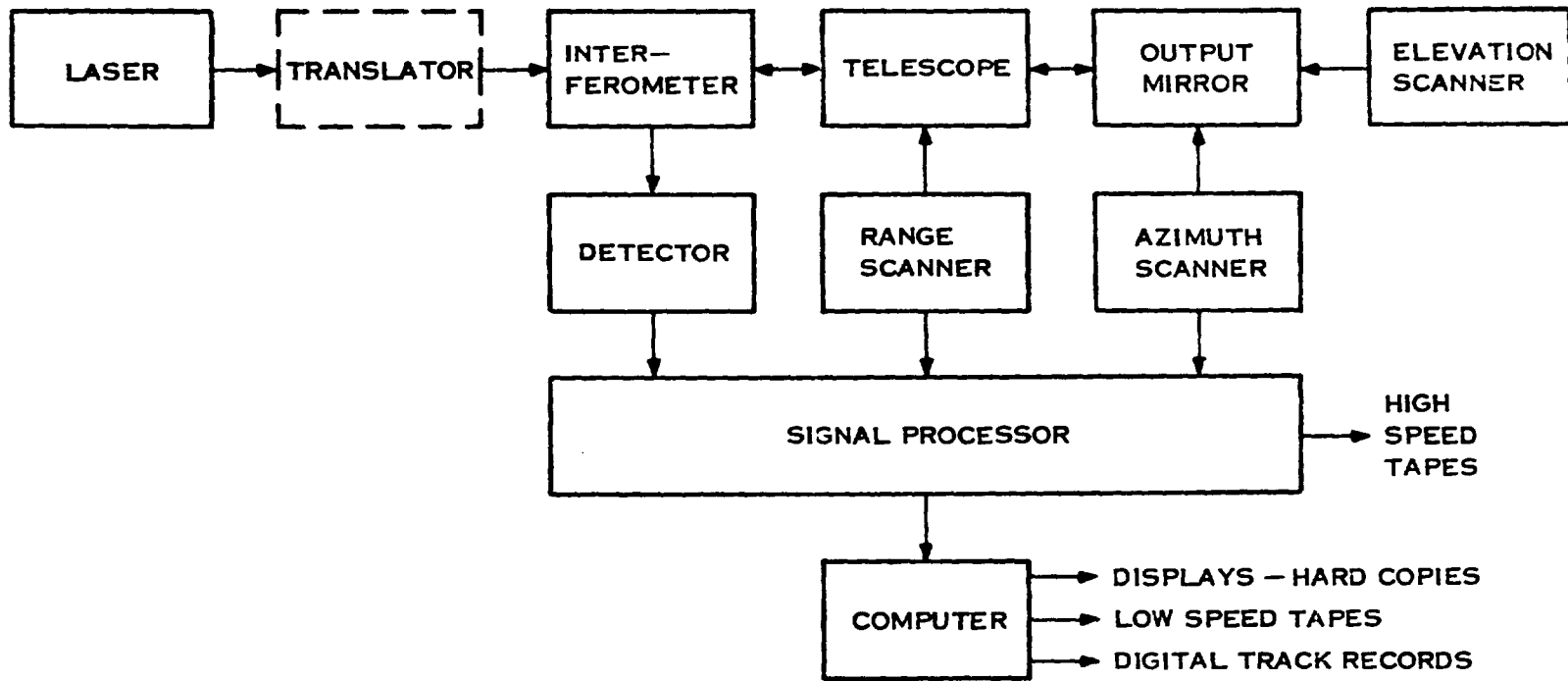


Figure 1-6. SLDV Block Diagram.



Figure 1-7. Overall Diagram of the SLDVS.

1-13

RAYTHEON COMPANY  
EQUIPMENT DIVISION



G:75:11

### 1.2.3 DUST DEVILS

Dust Devils are naturally occurring atmospheric vortices common in deserts, such as those in the southwestern United States. They vary in diameter from a few meters to tens of meters, and in altitude from 30 to several hundred meters. They are most frequently seen on hot, cloudless days in the early afternoon when the ground temperature is highest. The peak velocities vary from about 3 to 15 meters per second and the direction of rotation is apparently random. The principle reason for measuring dust devils with the SLDV is to determine the feasibility of using the system for measuring tornado-like flows.

The system is configured in a similar way to the vortex detection configuration with the addition of an azimuth scan. Thus, scanning in azimuth, the dust devil detection problem becomes almost identical to that of wake vortices. A typical scan configuration at Gila River Indian Reservation is shown in Figure 1-8.

### 1.2.4 DATA ANALYSIS

The data analysis served a number of purposes. It was used for diagnostic purposes, algorithm development, and vortex flow field analysis. Also, the programs were modified to analyze the dust devil data. The main program used in the data analysis was the LDV data processing algorithm which performs thresholding on each spectrum, locates vortices using a centroid on the highest amplitude in the spectrum and produces data files for use in flow field analysis.

The program used velocity and amplitude thresholds to remove noise and low velocities as shown in Figure 1-9. The following parameters were defined in the spectrum as shown:

- $I_{pk}$ , the highest amplitude in the thresholded spectrum,
- $V_{max}$ , the velocity associated with  $I_{pk}$ ,
- $V_{pk}$ , the highest velocity above the amplitude threshold,
- $S$ , the integrated signal, and
- $N$  the width of the thresholded spectrum.

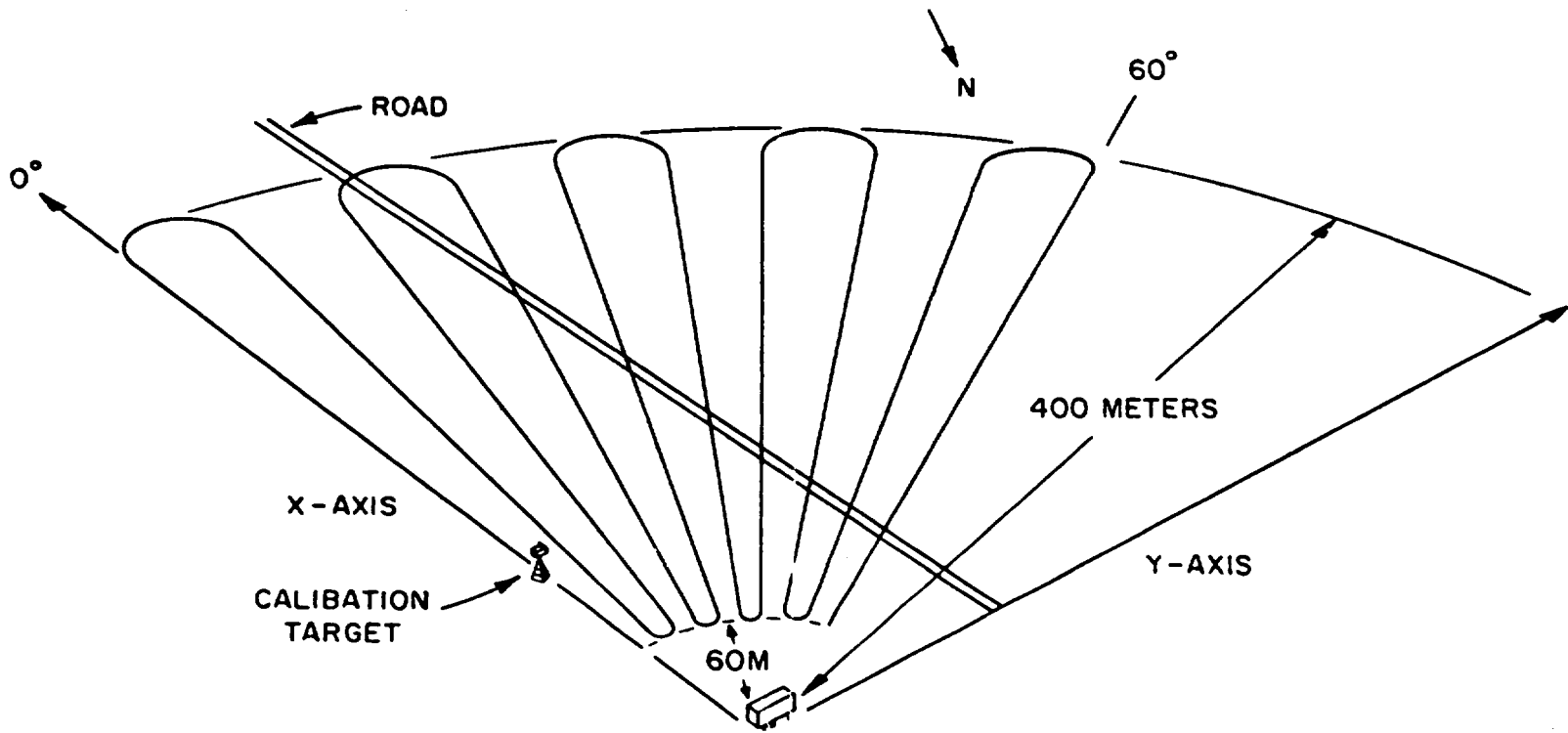


Figure 1-8. Gila River Indian Reservation Test Site.

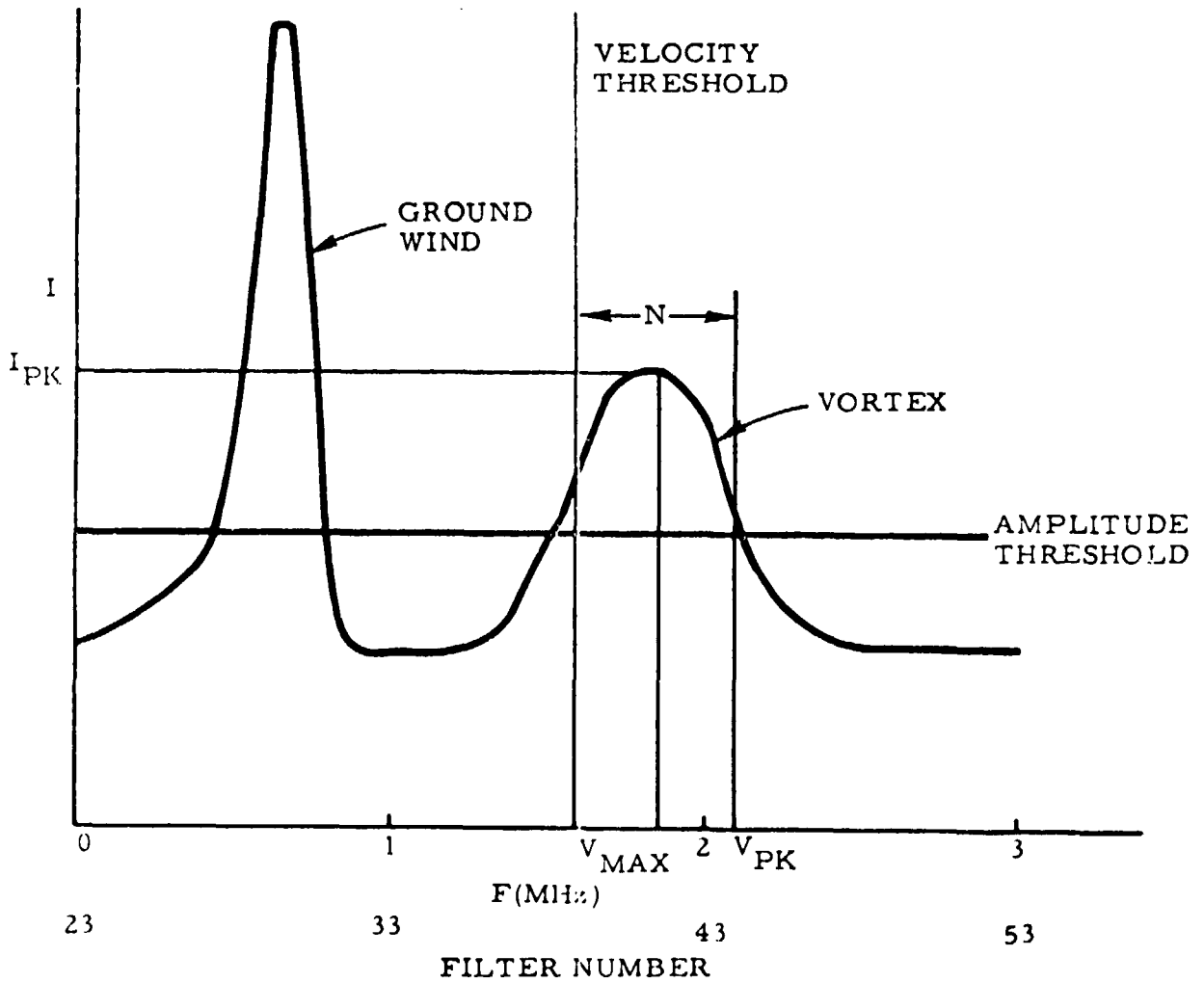


Figure 1-9. Vortex Signal Spectrum (Untranslated).

A new spectrum was obtained during each integration time (typically 2 msec for vortex studies and 8 msec for dust devils). Along with the above parameters, the range, angle, x and y coordinates, time, and a frame number were recorded.

For each scan, the maximum values of  $V_{pk}$ ,  $V_{max}$ ,  $I_{pk}$ , and  $S$ , and the average value of  $S$  were recorded. Also, location of the vortices was performed using an iterated centroid method. The location of one vortex was determined by locating the highest  $I_{pk}$ , considering all of the points falling within a correlation circle of specified radius of this point, and calculating the centroid, weighted with the amplitude above the threshold. A similar procedure was used to determine if a second vortex was present using the highest  $I_{pk}$  outside of the correlation circle defined for the first one, as the center for a new correlation circle. Points occurring in both circles were considered to be associated with both vortices for purposes of the centroid. The locations thus determined were used as centers for new centroids. If a majority of the points in either vortex was in the overlap region, the point which initiated the location of the second was deleted and the iteration procedure was begun again. The X and Y locations of each center were printed out after each stage of the iteration.

A number of other programs were used to translate tapes to CDC-6700 format, to print and plot the raw data, to analyze calibration runs, and to analyze vortex and dust devil flow fields.

Initially the data analysis effort concentrated on diagnostic applications such as evaluating signal-to-noise ratios and range resolution. Problems were located with the range scanners using raw data from both vans. The system was evaluated by testing it on the flow field from an aircraft engine to determine system performance and to evaluate algorithms for flow field location. Preliminary tests

were performed on aircraft vortices from a B-720 and B-737. From these, algorithm modifications were suggested for both real time and post analysis. At the same time, a simulation was used to evaluate potential algorithm improvements. During the tests at Kennedy International Airport, several runs were evaluated in post analysis and the quality of the real time data was studied. Suggested parameters for the algorithm were tested and modified leading to reliable real time vortex location. Also, the accuracy of the real time data was checked against the high speed data tapes and some minor problems were located and corrected.

Later during the Kennedy International Airport tests, a series of high altitude flybys using a C-880 was evaluated in real time. It was determined that the system could detect and track vortices at ranges up to 1500 feet. During the entire period, evaluations of system, operator, and algorithm performance were made. A program to determine effective circulation of vortices was developed, and tested. This program produced good results after the initial 10 or 15 seconds. The failure during the early part of the run was attributed to multiple vortices which are significant in a landing configuration. Spectra were used to determine the presence of multiple vortices and it was suggested that a wide spectrum with multiple peaks might be an indication of the presence of multiple vortices.

During the dust devil tests, real time data was evaluated and several runs with and without the frequency translator were processed. It was determined that in post-analysis, good transport and velocity profiles could be obtained.

In summary, the SLDV has been shown to be reliable in detecting, tracking, and monitoring aircraft wake vortices and naturally occurring vortices of widely differing sizes, backscatter coefficients, and velocities. The detection and tracking functions are now possible in real time, while the detailed velocity profile monitoring require more data and presently should be performed in post-analysis using the PCM data.

## SECTION 2

## VORTEX TIME HISTORIES

2.1 INTRODUCTION

The LDV data processing algorithm produces time histories of vortex parameters including x and y coordinates of centers, velocity profiles, scatter plots, maximum values of spectral parameters and other data for vortex analysis. These may be used to produce transport plots, backscatter and peak velocity time histories and vortex flow field studies. This section describes the algorithm briefly and shows results obtained on several runs.

2.2 DATA PROCESSING ALGORITHM

The LDV data processing algorithm performs the functions of vortex location and generation of data for additional analysis. The vortex location is established using the triplet  $I_{pk}$  algorithm described in the Interim Reports <sup>(4)</sup> dated 16 December 1974 and 3 November 1975. <sup>(5)</sup> In essence, the location is determined by locating centroids of  $I_{pk}$ . The algorithm also obtains the highest  $V_{pk}$ ,  $V_{max}$ ,  $I_{pk}$ , and integrated signal and the average signal in each scan, and provides time histories of these. Additionally, scatter plots are generated for  $V_{pk}$ ,  $V_{max}$ ,  $I_{pk}$ , and the integrated signal. Finally, a velocity vs. angle plot is constructed for each vortex in each scan, for use in determining the flow field parameters.

2.3 RESULTS

Several runs have been analyzed using the LDV Data Processing Algorithm. Transport results are generally in good agreement with those obtained in real time as expected. A sample of the vortex transport results is shown in Figure 2-1. The numbers represent scan numbers and show the locations of vortices over the first 20 seconds of the run. The aircraft was a DC-10 and the tower was reporting winds of 7 knots at  $350^{\circ}$  resulting in a cross-wind of



VORTEX TRANSPORT PLOT  
 RUN 1051 SEQ 0133  
 DAY 127 PLOT REVISION 2.04  
 REEL 1

RAYTHEON COMPANY  
 EQUIPMENT DIVISION



2-2

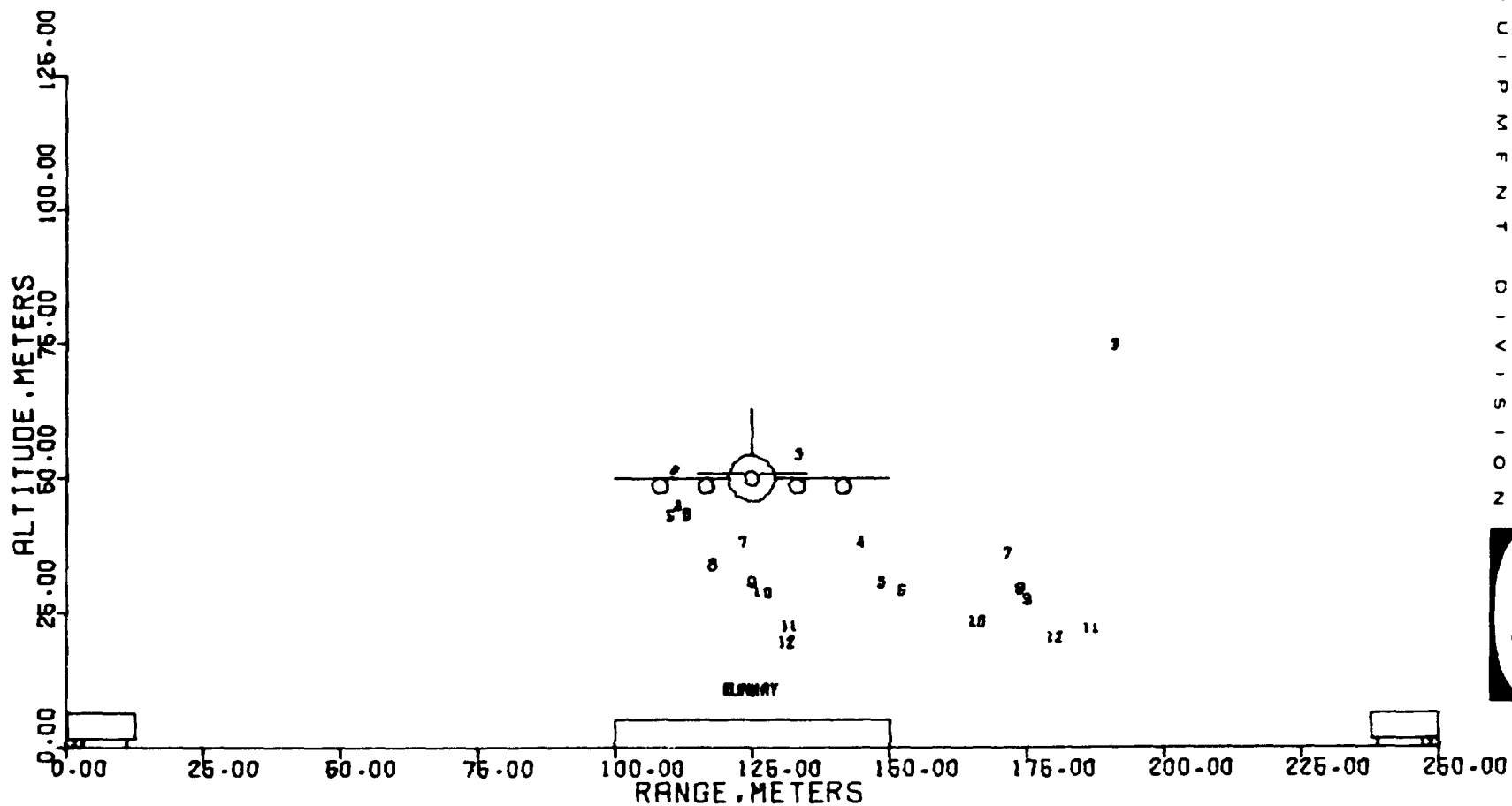


Figure 2-1. Sample Vortex Transport.

7.6 ft/sec away from Van 1. This run will be discussed in greater detail later by comparing the transport to the wind measured from a meteorological tower. In Figure 2-2, a composite of two data tapes shows 40 seconds of data on a B-747 vortex in a light wind. Some evidence of a shear and the effect of ground interaction are clearly evident. A similar composite for a DC-8 in a moderate crosswind is shown in Figure 2-3. This shows both vortices being transported toward the van, apparently due to the crosswind which was determined from tower data as 17 ft/sec.

The change of spectral parameters with time is also of interest. Generally, the highest  $V_{pk}$  and  $V_{max}$  per scan are nearly equal and vary during the run from about 15 m/sec (50 cells or 50 ft/sec) down to the threshold at about .3 ft/sec<sup>2</sup>. Sometimes  $I_{pk}$  also shows a reduction during the run corresponding to 10 dB or more over the duration of the run. In other cases this is less apparent, and in at least one case, a growth in  $I_{pk}$  can be seen. Figure 2-4 shows the results for a B-747 in a moderate wind while Figure 2-5 is for a DC-9 in a high wind. It is interesting to note the similarity of the  $V_{pk}$  and  $V_{max}$  time histories from very different aircraft. The  $I_{pk}$  time histories are very different, and may reflect the different amount of exhaust from these aircraft. The DC-9 having only 2 small engines may contribute little enough to  $I_{pk}$  so that ambient atmospheric effects are significant. On most runs, the  $V_{pk}$ ,  $V_{max}$  behaviors are similar to those shown and in most cases, some overall decrease in  $I_{pk}$  can be seen.

#### 2.4 TRANSPORT VS. WIND COMPARISON

The transport was compared to the components of the wind velocity for four runs. The wind velocity components were measured by sensors mounted on meteorological tower 1, located between the middle marker and runway 22L-4R. Run 2011 (Day 126) shows a DC-8 vortex pair being horizontally transported toward Van 1 at about 17 ft/sec. The measured crosswind components were  $13.09 \pm 1.26$  ft/sec at 40 ft altitude and  $11.42 \pm 1.63$  ft/sec at 20 ft. Additionally,

VORTEX TRANSPORT PLOT  
 RUN 2011  
 DAY 118

PLOT REVISION 2.04

2-4

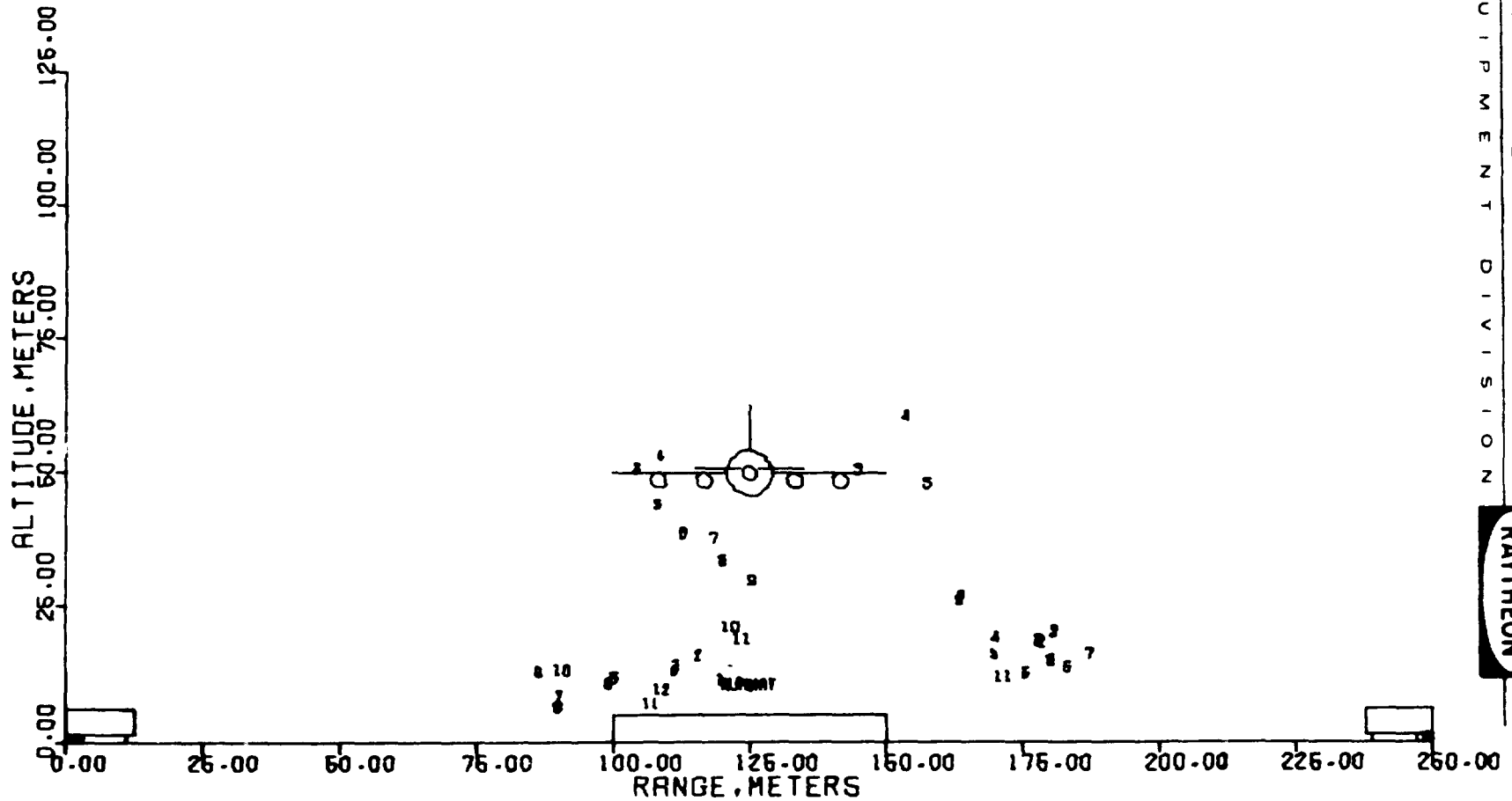


Figure 2-2. Sample Vortex Transport.

VORTEX TRANSPORT PLOT  
 RUN 2035  
 DAY 115

PLOT REVISION 2.04

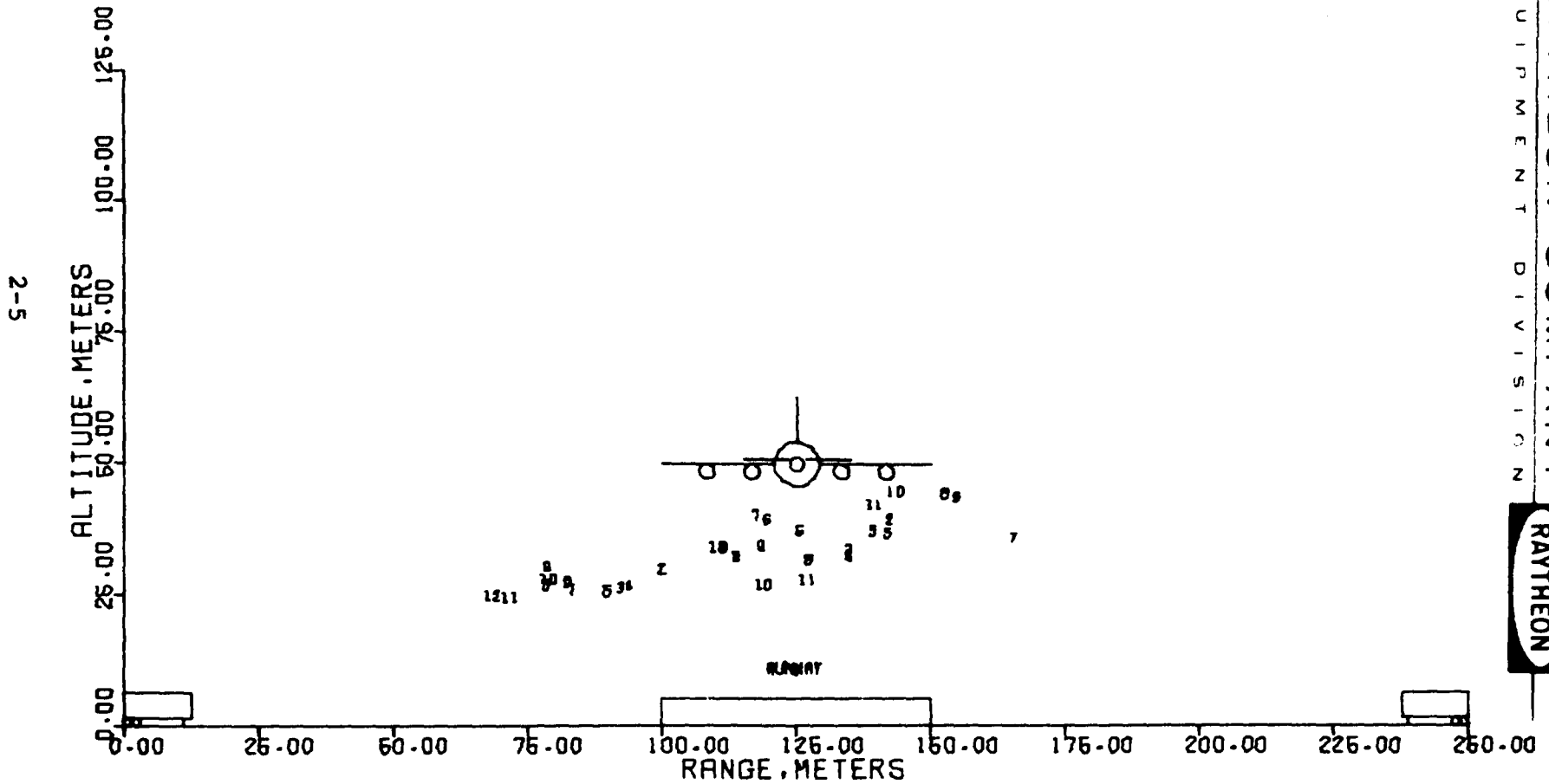
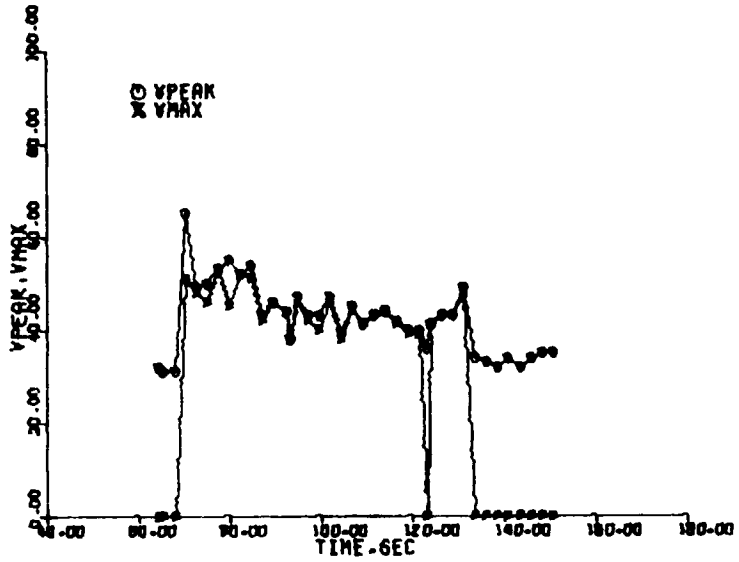


Figure 2-3. Sample Vortex Transport.



ISEQ 117 DAY 115 RUN 2019  
PLOT REVISION 2-04 START TIME =48100 SEC

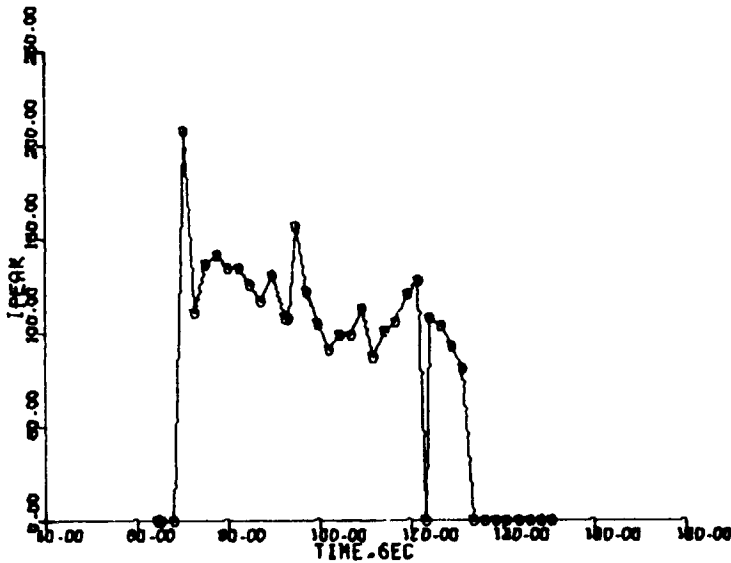
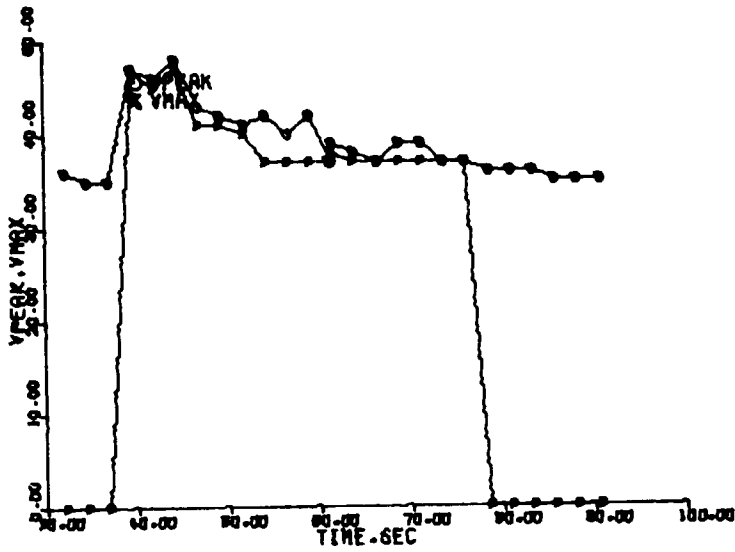


Figure 2-4. Parameter Time History.



ISEQ 120 DAY 118 RUN 2020  
PLOT REVISION 2.04 START TIME = 63900 SEC

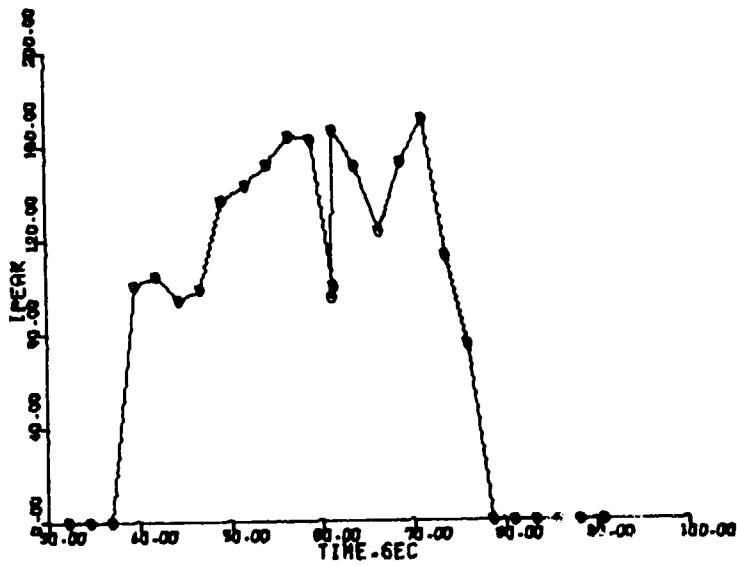


Figure 2-5. Parameter Time History.

there was a 3.3 and 3.5 ft/sec tailwind at the two altitudes and a .44 ft/sec upward component at 40 feet. The vortex was observed until it left the scan plane at about 60 feet altitude. The crosswind velocity values and vortex transport are consistent with a slight shear in the form of a slightly increasing crosswind with increasing altitude.

Run 1031 (Day 127) shows a vortex pair from an L-1011 being transported at about -10 ft/sec per second. After 15 seconds, one vortex left the scan plane. The other continued to fall and changed its velocity until it was traveling in the opposite direction at an altitude of about 40 feet. After that it rose in altitude and returned to its original transport for the rest of the 75 seconds for which it was observed. The measured crosswind was -6.00 ft/sec at 40 ft. altitude and -.66 ft/sec at 20 ft. This run shows evidence of a shear going from -10 ft/sec at 150 ft. to 0 at the ground. The wind velocity may reverse near the minimum altitude of the vortex or the reversal of transport velocity may be due to the induced velocity caused by ground effect. A headwind of 12 to 13 ft/sec was observed on this run.

Run 1051 (Day 127) was a DC-10 aircraft landing in a 10 to 11 ft/sec headwind. The horizontal transport velocity of this vortex pair was nearly uniform at approximately -5.7 ft/sec down to an altitude of about 50 ft., in agreement with the crosswind velocity at 40 ft. The crosswind at 20 ft. was -7.8 ft/sec.

Run 1055 (Day 127) was another DC-10 landing in a 12 ft/sec headwind. The vortex horizontal transport was fairly uniform at about -12.5 ft/sec down to an altitude of 75 ft. The crosswind was -7.21 ft/sec at 40 ft. and almost 0 at 20 ft.

It is difficult to make a quantitative estimate of the correlation between vortex transport and wind data since the wind data is taken from a 40 foot tower while the vortices are seldom at that low an altitude. Furthermore, when the vortices descend to 40 or 50 feet, the effect of ground interaction becomes significant. The assumption

that the vortex transports with the local near wind does lead to realistic profiles of a wind shear. Vortex transport and anemometer data are summarized in Figure 2-6.

## 2.5 CONCLUSIONS

The study of vortex time histories has produced a number of results. First, it led to improvements in the real time data processing. Later, whether real time analysis was producing good results, the emphasis of post-analysis shifted to obtaining more details concerning the vortices and the system. In particular, sub-routines were included to process the data to aid in flow field studies and spectral parameter time histories.

The peak velocity vs. time behavior is very repeatable, even for different aircraft, with typical peak velocities in the neighborhood of 15 m/sec. at the beginning of a run. Transport data are in good agreement with those obtained in real time and reflect the velocity of the local wind and induced velocities from the interaction of the vortices and the ground.





Key: V = Vortex Horizontal Transport  
A = Anemometer Cross-wind Velocity

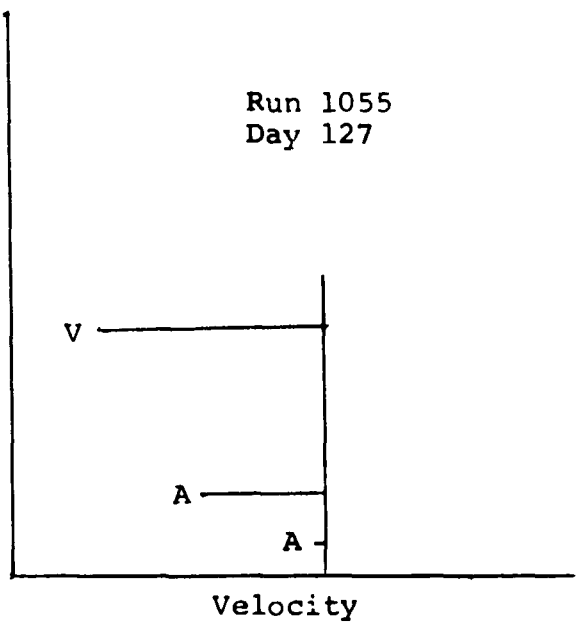
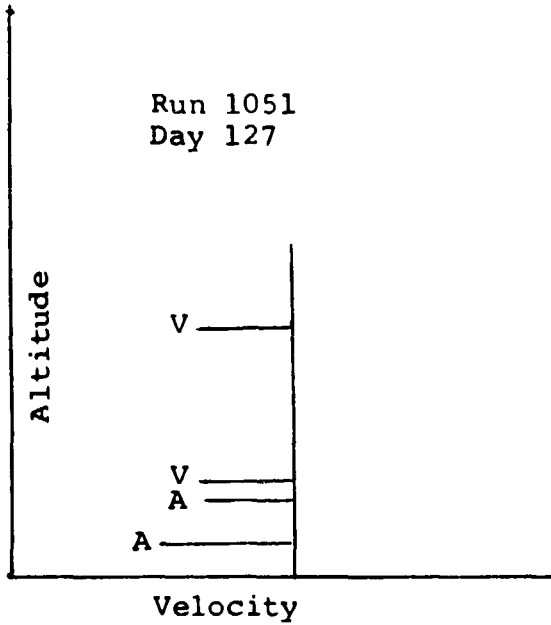
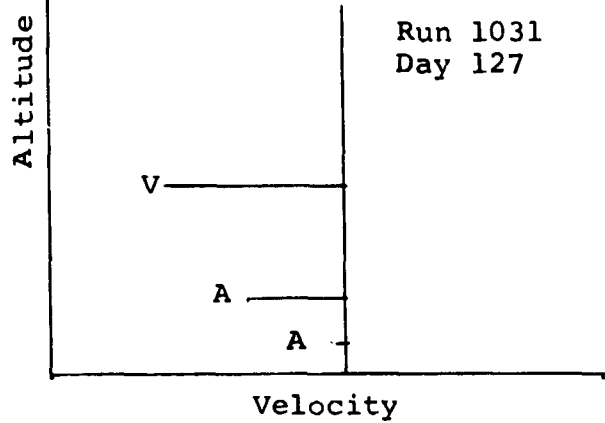
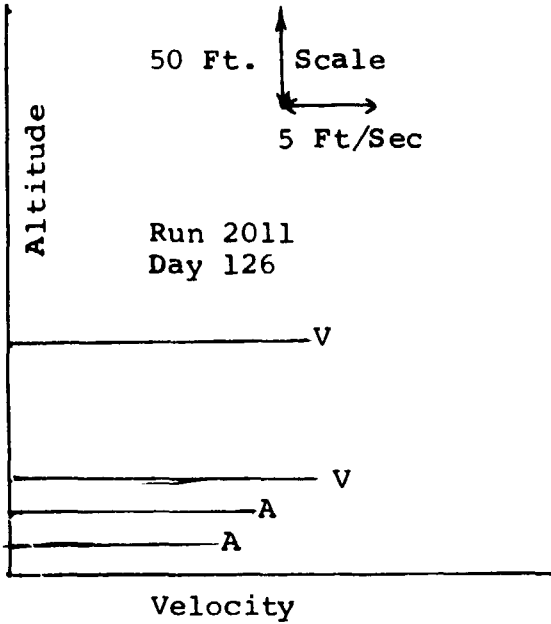


Figure 2-6. Vortex Transport - Wind Profile Comparison.

SECTION 3

EFFECTIVE CIRCULATION CALCULATIONS

3.1 INTRODUCTION

The effective circulation of a vortex is defined in terms of the circulation of a model vortex. The model postulates that the circulation is constant and that the rolling moment on a hypothetical following aircraft of wingspan  $b$  is equal to  $\Gamma b/2\pi$ .

The actual data is processed to determine the rolling moment  $M$  as a function of  $b$ . This function usually curves upward from the origin into a linear region followed by a saturation outside the region of the vortex. The effective circulation is defined as  $2\pi$  times the slope  $\frac{dM}{db}$  in the linear region. Using this method, twelve runs have been processed to determine the effective circulation as a function of time for each of the vortices. Unexpectedly high values of circulation are obtained in the early scans of most runs and it is postulated that these are due to the presence of multiple vortices.

In this section, the methods of calculating effective circulation are described, followed by a few examples and a summary of the results.

3.2 METHODS OF CALCULATION

The effective circulation of a vortex may be calculated from the LDV data in one of three ways. All approaches make use of plots of the peak velocity vs. angle. These plots are restricted to include the vortex of interest by including only data collected with ranges within 10 meters of the vortex range. Thus, two velocity vs. angle plots are generated for each scan (if two vortices are present). Each plot contains data from a 20 meter range bin centered at the vortex range as shown in Figure 3-1. The highest velocity in the spectrum at each point is assumed to be the velocity of the vortex along the given line-of-sight.

Since no frequency translation was used in collecting the data, it was necessary to locate the center of the vortex in angle and

assume that a sign change occurred at this point. The center was located by finding two angles having high velocities and having a relative minimum velocity between them. The two peaks were assumed to correspond to the two sides of the core while the null was identified as the angular location of the vortex center.

The easiest circulation estimate is obtained by selecting a point on the velocity vs. angle plot, determining its radial distance from the center (using the angles and range), and calculating

$$\Gamma = 2\pi Vr$$

where  $r$  is the radial distance to the vortex center  
 $V$  is the peak velocity at that point

This method has the advantage of being easy and the disadvantage of using very little of the data. Furthermore, it is not necessarily related to any wake effects which would be experienced by an encountering aircraft.

The second approach is a least square fit to an assumed vortex model with variable parameters. Measured data is used to obtain the best values for these parameters, and then the model may be used to calculate the circulation. This method makes use of more of the data, but, again, does not necessarily relate to the effect on an encountering aircraft, since the calculated circulation is dependent on the model chosen.

The third approach, the rolling moment method, makes use of all the data and produces a circulation estimate which is significant to the encountering aircraft. The procedure is to calculate the rolling moment on a hypothetical aircraft of wingspan  $b$ , using the LDV data:

$$M = \int_{-b/2}^{b/2} v \cdot r \, dr$$



This quantity, in the constant circulation model of a vortex, is proportional to the wingspan in such a way that the circulation is

$$\Gamma = 2\pi \frac{dM}{db}$$

For an actual vortex, this equation will not hold for all values of  $b$ . However, it is possible to determine an effective circulation by applying this equation in a region where the  $M$  vs.  $b$  curve is linear. This method has produced good results in moderate crosswinds for vortices at least 10 to 15 seconds old.

### 3.3 RESULTS

The effective circulation calculation has been performed using the rolling moment method on wake vortices from a variety of aircraft types in different wind conditions. The calculation has been performed on each vortex for every scan in several runs, to produce a time history of effective circulation for each vortex. An example for a B-747 is shown in Figure 3-2.

The B-747 results indicate that reasonable values are obtained after 10 seconds in both low and moderate crosswinds. Most of the results for run 1019, on day 115, are lower than the expected values and the results of the other B-747 runs. This may be due to the use of too high an amplitude threshold. A few scans produced reasonable results and these are in good agreement with the results from van 2. Both runs 2011 (day 118) and 2019 (day 115) produced high effective circulation in the first few scans. The L-1011 results show similar behavior with circulation somewhat high in the first few scans. The DC-8 results in low to moderate crosswinds also behave in a similar fashion, while the high crosswind run has an effective circulation which is too high throughout most of the run. This may be due to changes in the vortex velocity due to the wind, which do not cancel out, because of the folding of the LDV spectrum about zero.

With three runs processed earlier, the overall result of the effective circulation calculations include usable data on 10 out of 12 runs. There is considerable scatter in some of the data, but the overall trends are readily apparent. It has been determined that effective circulation calculations are relatively sensitive to the amplitude threshold, and that the optimum threshold for these calculations is not always the same as the optimum for vortex location.

### 3.4 CONCLUSIONS

The rolling moment method usually produces reasonable values of effective circulation which may be used as a measure of vortex strength. The calculations have been performed for every scan of several runs lasting up to 60 seconds. The effects of low to moderate crosswinds have been previously shown to be small, as have errors in locating the vortex center. Any study of flow field parameter would be simplified by the use of a frequency translator.

It has been determined that the effective circulation calculation is quite sensitive to the amplitude threshold and that the optimum threshold may be different for vortex location and effective circulation calculation. For the latter, the threshold should be as close to the noise floor as possible without causing a high false alarm rate.

Finally, it has been observed that the effective circulation is almost always too high during the first few scans. This is probably due to the existence of multiple vortices which will be discussed in the next section.

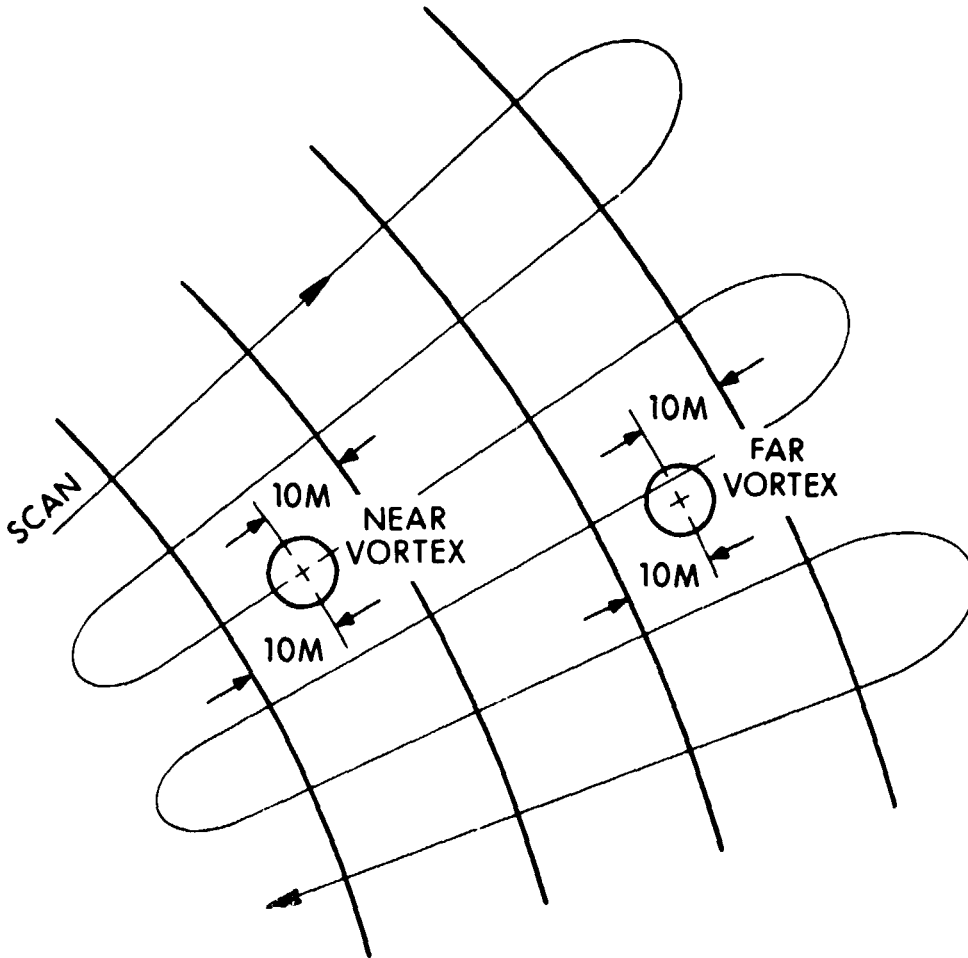


Figure 3-1. Method of Selecting Points For Velocity Profiles.

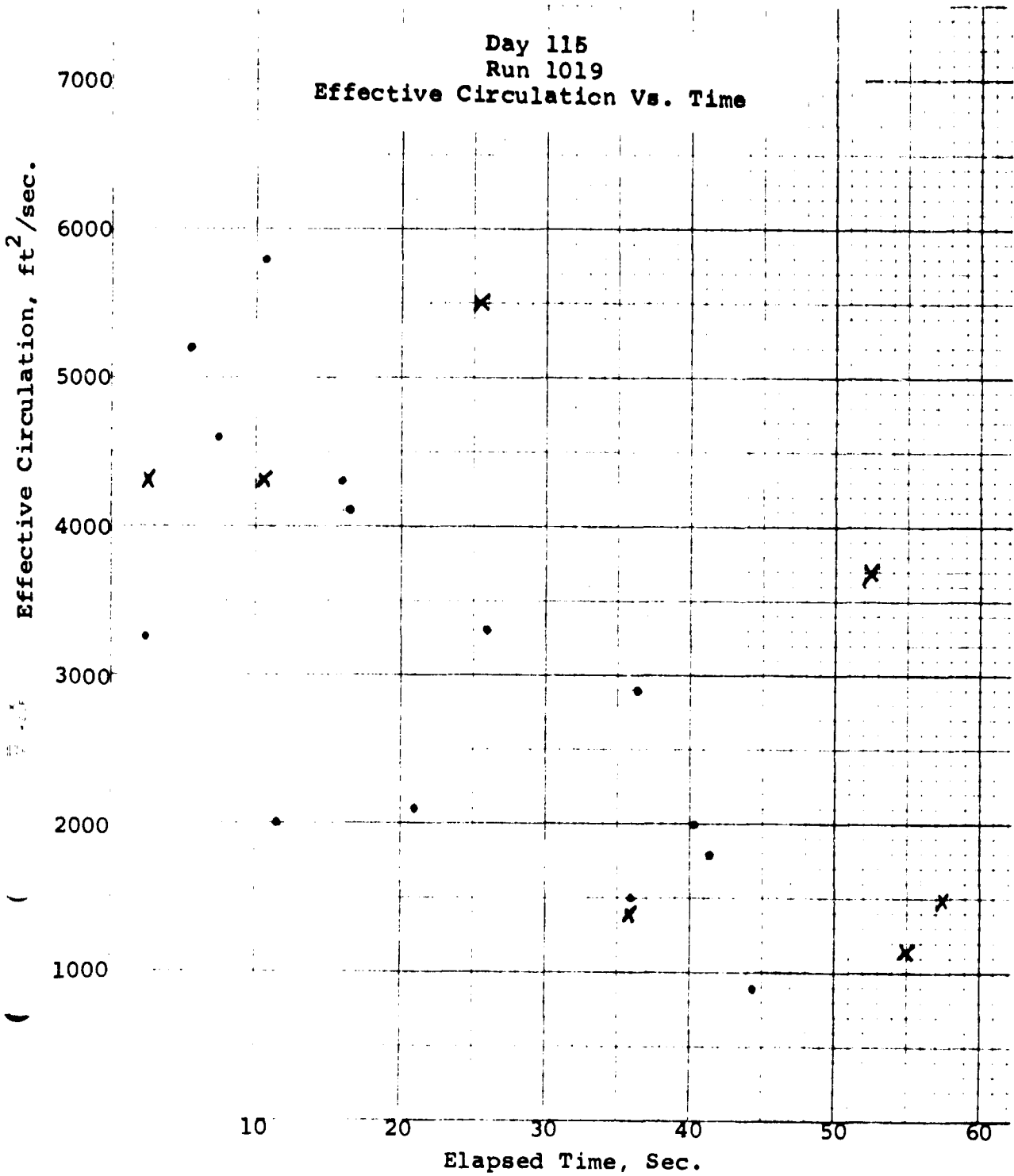


Figure 3-2. Effective Circulation Vs. Time for B-747 Vortices in a Category II Wind.

## SECTION 4

### MULTIPLE VORTICES

#### 4.1 INTRODUCTION

The study of multiple vortices has become of interest for a number of reasons. First, experimental and theoretical studies have been undertaken to determine if multiple vortices can be made to interfere, producing a vortex system which decays more rapidly than those in present aircraft wakes. Additionally, several phenomena observed in the KIA data are difficult to interpret on the basis of a simple vortex-pair model. In particular, excessive effective circulations have usually been obtained during the first ten seconds after vortex generation.

Work performed on the KIA data has indicated that multiple vortices may be studied by using spectral analysis and velocity vs. angle plots. Lifetimes of multiple vortex systems have been estimated at 10 to 20 seconds based on observations of spectra, velocity profiles, and effective circulation results. After this time, the vortices apparently merge into a well defined vortex pair.

Multiple vortex study may yield a further understanding of the seemingly erratic behavior of vortex system characteristics such as transport and decay as well as providing means to develop methods for reducing vortex lifetimes and strengths.

#### 4.2 MODELS

The initial number and location of vortices in an aircraft wake are strongly dependent on the type of aircraft and the flap setting. In the cruise configuration, the flaps are fully retracted, resulting in a smooth wing surface which generally produces only a pair of counter-rotating wingtip vortices, separated by about 3/4 of the wingspan. However, in the approach and landing configurations, the flaps are extended, and vortices are generated wherever there is a discontinuity in the wing surface; namely at all flap edges and





at the wing tip. For aircraft with segmented flaps, such as the B-747, L-1011, DC-10, and B-727, as many as ten vortices may be generated when the flaps are deployed. For these aircraft in the landing configuration, the strongest vortices arise at the outer edges of the outer flap segments, and the transport of a young vortex system is most strongly dependent on that vortex pair.

For the aircraft investigated by Snedeker and Bilanin<sup>(1)</sup>, the strongest vortex circulation strength and location are tabulated in Table 4-1. These results lead to a straightforward calculation of

TABLE 4-1

Multiple Vortex Data  
for Landing Configuration

Aircraft	Number of Vortices Per Wing	Strongest Vortex Location (a)	Vortex Circulation Strength	Calculated Descent Rate (b)	Next Highest Circulation Strength (c)
B-747	5	68 ft.	4663 ft <sup>2</sup> /sec	5.5 ft <sup>2</sup> /sec	.6875
L-1011	4	60 ft.	2912 ft <sup>2</sup> /sec	3.9 ft <sup>2</sup> /sec	.7977
DC-10	3	58 ft.	2514 ft <sup>2</sup> /sec	3.4 ft <sup>2</sup> /sec	.5740
B-727	4	41 ft.	2261 ft <sup>2</sup> /sec	4.4 ft <sup>2</sup> /sec	.7939

- (a) Strongest vortex generated at outside of outside flap in all cases. Location is from aircraft centerline.
- (b) Based on strongest vortex only.
- (c) Expressed as a fraction of strongest vortex circulation.

---

(1) Richard S. Snedeker and Alan J. Bilanin "Analysis of the Vortex Wakes of the Boeing 727, Lockheed L-1011, McDonnell Douglas DC-10, and Boeing 747 Aircraft", Final Report dated July 1975 (Contract #DOT-TSC 845)

the descent rate, if only the two outboard flap vortices are considered:

$$-\frac{dy}{dt} = \frac{\Gamma}{2\pi b'}$$

where

$\Gamma$  is the circulation strength and

$b'$  is the separation between the two vortices.

In addition, the second-strongest vortex was found, and the ratio of its circulation strength to that of the strongest is included. This provides a measure of the error introduced by considering only outboard flap vortices.

When the SLDV system scans through a complicated multiple vortex system, the result will be an increase in the complexity of both the spectra and velocity profiles. For a system without a frequency offset, these will be further complicated by the folding of the spectra. With the range resolution possible at reasonable ranges, the focal volume of the SLDV must include several vortices, which may be expected to result in an increase in the width of the spectrum and the appearance of multiple peaks. The interpretation of these behaviors is complicated by spatial variations in the back-scatter coefficient.

It is generally believed that after a period of time, vortex merging takes place and reduces the complicated vortex system to a simple pair of counter-rotating vortices. Observation of experimental data for multiple vortex effects should thus be concentrated on the first 10 seconds after generation. Finally, it should be noted that, for large aircraft, the effect of ground interaction may be significant.

### 4.3 EXPERIMENTAL RESULTS

#### 4.3.1 INTRODUCTION

The presence of multiple vortices in young aircraft wakes is

indicated by several experimental results. These include changes in the spectral characteristics and velocity profiles, as well as effects on the descent rates and effective circulation calculations. Some of these results have other potential explanations in addition to multiple vortices, but the combination of all the results indicates strongly that multiple vortices are significant during the first 10 to 20 seconds after aircraft penetration.

#### 4.3.2 SPECTRA

The spectral characteristics of an aircraft wake change with time. The spectra of young wakes typically contain high velocities, have wide bandwidths and often exhibit multiple peaks with deep nulls between them. The spectrum is clearly that of a complicated velocity and/or backscatter coefficient distribution rather than that of a simple vortex in a uniform atmosphere. Typical peak velocities are on the order of 15 m/sec. Often significant signals are obtained at all velocities between 2 to 5 m/sec and 15 m/sec resulting in a signal bandwidth of close to 3 MHz.

These spectra typically have a number of peaks and valleys indicating that there is significant backscatter from several regions of different velocities. This may arise in one of two ways. First, for a single vortex, locally high concentration of particulate in small regions may be moved about by the vortex flow field. Their velocity components would differ because of their different locations within the vortex. If this is the case, the ratio between peaks and nulls should be equal to the ratio of maximum to minimum backscatter coefficient along the line of sight. This has been measured to be as high as 18 dB (day 115, run 2019, frame 5918), which seems excessive, based on this explanation. The other possibility is that the velocity component along the line of sight undergoes irregular changes as would be the case if the line of sight penetrated several vortices.

As the wake ages, a number of changes occur in the spectra. Most notably, the peak velocity falls, more or less smoothly by about 2 to 3 meters per second in 20 seconds, and continues to fall throughout the life of the wake. The peak velocity usually falls below a threshold of 5 m/sec about 60 to 90 seconds after vortex generation. Typical vortex spectra are shown in Figure 4-1. These were obtained with the wake of a B-747 in a wind reported to be from  $20^{\circ}$  at 5 knots. Samples of a young wake spectrum immediately after generation and an older wake (about 20 seconds later) are shown. The characteristic broadening, high peak velocity and multiple peaks are clearly evident in the young wake spectra, while these phenomena are greatly reduced after 20 seconds.

#### 4.3.3 MULTIPLE VORTEX VELOCITY PROFILES

Evidence of multiple vortices is also apparent on some occasions in plots of the vortex velocity component as functions of angle. A detailed analysis of the multiple vortex problem is not possible with this data, due to the low angular data density available. The finger density in a typical finger scan is approximately one point per degree. For a B-747 aircraft approaching the runway at 50 meters altitude, a typical scan pattern is shown in Figure 4-2. Measuring  $V_{pk}$ , the highest velocity component along the line of sight, approximately 8 independent values may be obtained over an area corresponding to one wing. These will obviously not be sufficient to determine the locations and velocity flow fields of five vortices. However, it should be apparent whether or not the velocity profile is more complicated than that of a single vortex.

A sequence of several velocity profiles is shown in Figures 4- through 4- . These show  $V_{pk}$  as a function of angle for data points having ranges within ten meters of the vortex range as determined by the vortex location algorithm. It may be seen that considerable structure exists in the early profiles. The details of this structure may not be readily related to the model vortices, since the evolution of the multiple vortex model results in a revolution

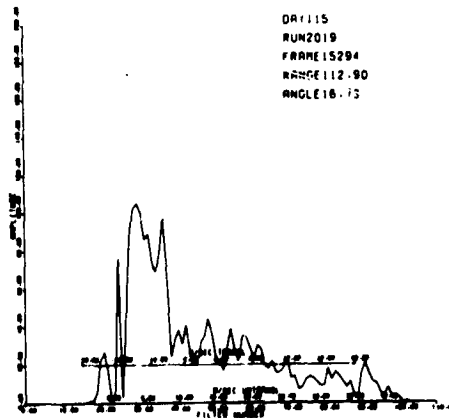
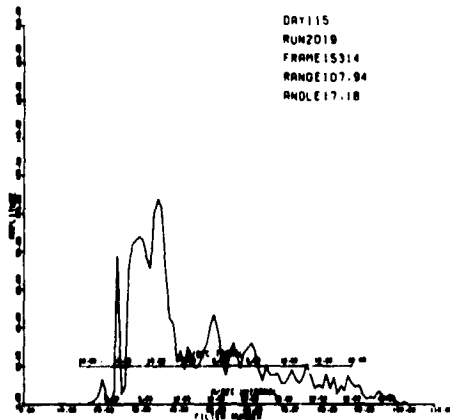
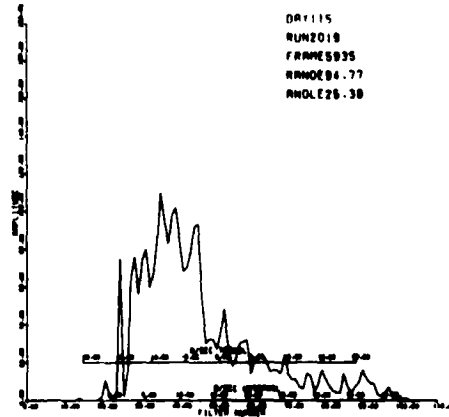
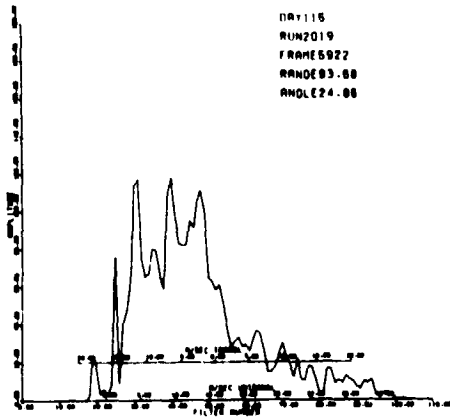


Figure 4-1. Typical Vortex Spectra.  
Top: Young Vortex System  
Bottom: Twenty Seconds Later



4-7

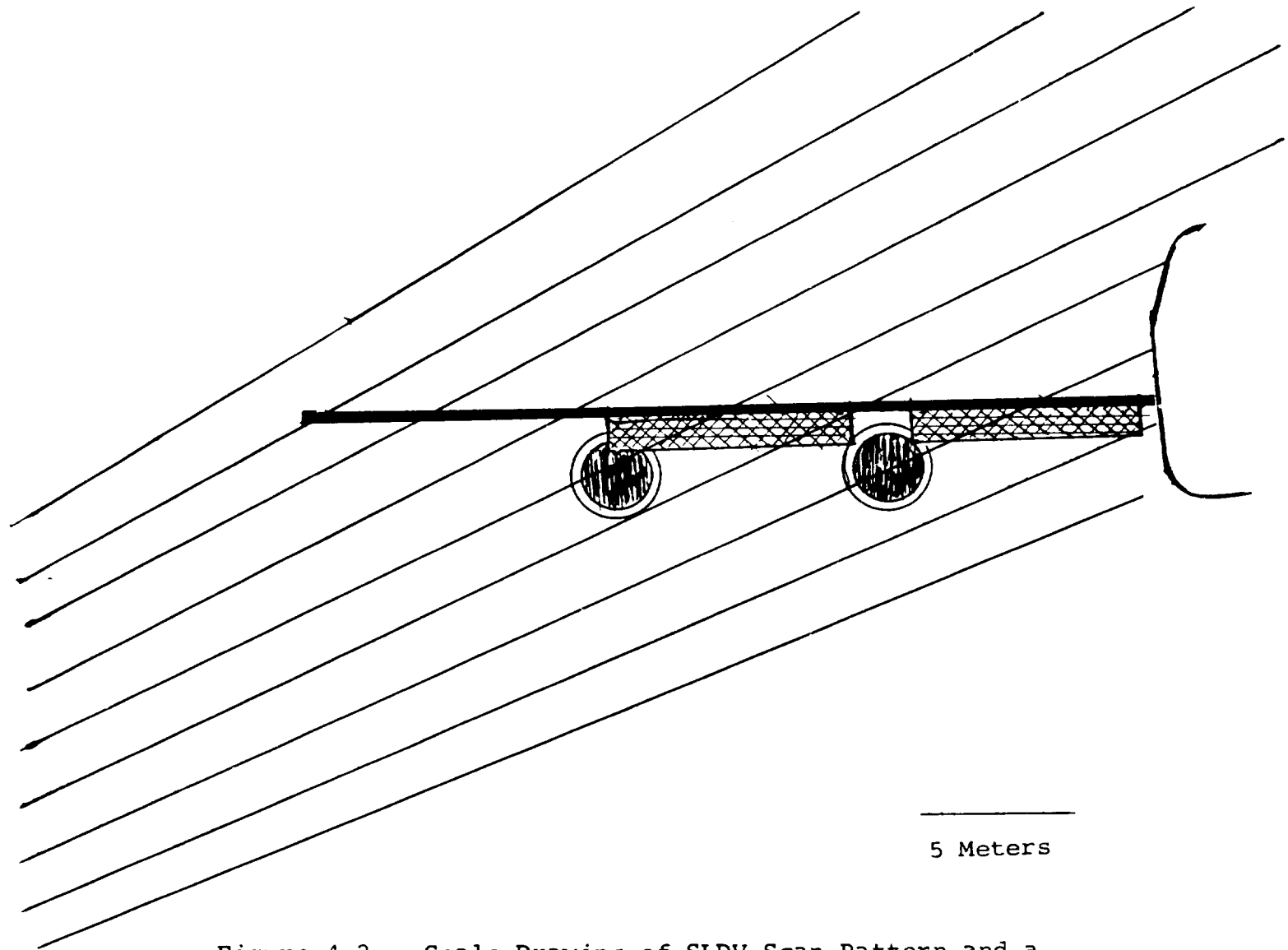


Figure 4.2. Scale Drawing of SLDV Scan Pattern and a B-747 Wing.

of some of the vortices about others. Thus, the exact angular profile depends on the exact time after generation and on details of the vortex flow field for the specific aircraft. Furthermore, it is not unreasonable to expect that the vortex locations change significantly during a scan, resulting in size and location errors. The detection of multiple vortices from velocity profiles would be aided considerably by using data from an arcscan performed at the correct range. The practical limits on mirror speed will probably preclude the possibility of "freezing" the motion of a multiple vortex system, but high data density and more sophisticated processing could result in a significant improvement over the data presently available.

#### 4.3.4 POTENTIAL EFFECTS OF MULTIPLE VORTICES ON VORTEX TIME HISTORIES

Three effects of multiple vortices may have impact on the vortex time histories. First, effective circulation and rolling moment calculations may result in erratic, excessively high answers since the measured velocities are being treated incorrectly. Secondly, the descent rate may be altered by the complicated interaction of a multiple vortex system. Finally, some transport fluctuations may occur.

The effective circulation has been determined by considering the functional dependence of the rolling moment induced on an hypothetical following aircraft on the windspan of that aircraft. Since the velocity information does not contain sense, it is necessary to make assumptions regarding the flow field. A single vortex is assumed and the sense of the velocity is assumed to change sign at the location of the best null in the velocity profile, which should correspond to the center of the vortex. For a more complicated system, there may be several changes in the sense of the velocity. Failure to consider these will always result in a rolling moment which is too high. It is also possible that at some time, the vortices within the range sample of interest will be aligned along the line of sight. In this case, for a measurement of  $V_{pk}$ , a masking of the weaker vortices by the stronger ones will occur.

Then the rolling moment and effective circulation will be reduced; possibly to the values corresponding to the strongest vortex in the range sample. These phenomena can result in fluctuations in the calculated effective circulation, with a strong tendency toward high values. In fact, this has been observed in most of the runs which have been processed. The effective circulation generally returns closer to anticipated values after about 10 to 15 seconds. This may be considered as an estimate of the length of time over which multiple vortices are significant.

Descent rates measured during tests at Kennedy International Airport indicate that vortices fall at a slower rate than predicted by simple theories. The effect of multiple vortex transport is difficult and has not been considered in detail. The simplest assumption is that the wake descent is dominated by the action of the strongest vortex pair; namely, the outboard flap vortices. A comparison of these calculations with experimental averages is shown in Table 4-2. It should be noted that the descent rates have not been corrected for the headwind velocity, which tends

TABLE 4-2

## DESCENT RATE COMPARISON

Aircraft	Calculated	Experimental
B-747	5.5 ft/sec	5.4 ft/sec
DC-10 and L-1011	3.6 (average)	4.5
B-727	4.4	5.3

to increase them. While the agreement is not excellent, it is better than that with the simpler, wingtip vortex theory. It is anticipated that interaction with the inboard flap vortices would improve the model.



Finally, revolution of the vortices about each other may lead to changes in the path length, along the line-of-sight, over which the velocity component corresponds to a given filter. This will introduce fluctuations into the spectral characteristics including  $I_{pk}$ , on which the location algorithm is based. These fluctuations may lead to location errors. It is anticipated that these errors should be small, since the fluctuations should be small, but the result could be a fluctuation in vortex range, as has been observed occasionally in the data.

#### 4.4 CONCLUSIONS

The presence of multiple vortices in the KIA data is indicated by spectral analysis, velocity profiles, effective circulation calculations and descent rates. The most promising means of studying multiple vortices is an arcscan with high angular data density and a short scan time. Using the existing data, the best approach would be a detailed spectral analysis considering the ratios of peaks and valleys in the spectra. This could yield some size and peak velocity data which would be compared to simple models. Evaluation of descent rates could also be useful if the models were processed to determine theoretical descent rates for comparison.

SECTION 5  
SYSTEM PERFORMANCE

The SLDV system performance has been excellently for detection of wake vortices in an airport environment, and atmospheric vortices such as dust devils. Detailed descriptions of system performance at each stage of the test period are given in each of the interim reports. This section presents a short summary of the results obtained in detail in those reports.

After some initial hardware problems were resolved in the preliminary tests at Marshall Space Flight Center and some software improvements and parameter optimization in the early tests at Kennedy International Airport, the system was proven reliable for detecting and tracking vortices in real time as well as for providing flow field data for later analysis. Vortex location accuracy was approximately 20% of the range resolution. This resulted in the ability to track vortices near the landing path with a 10 foot accuracy.

Signal-to-noise ratios for atmospheric wind and aircraft wakes varied from 20 dB to more than 30 dB, the change apparently caused by changes in particulate distribution. The system range resolution was found to agree with theoretical calculations, based on data from hard target (sandpaper disc) measurements. The range resolution at the target location, 170 meters from the van, was anticipated to be 19 meters, and on several occasions, values of less than 20 meters were obtained. It was observed that there was a tendency for the range calibration to change with time, so occasional checks and corrections are required for measurements requiring great accuracy in range location.

The use of a frequency translator has been demonstrated to be valuable in measurement of dust devils, although the particular one used apparently introduces a loss in signal-to-noise ratio. A frequency offset would significantly improve the usefulness of the system for multiple vortex studies since it would resolve some of the flow field ambiguities existing in the present system.

Three bad runs were processed to determine the problems associated with them. One Day 115, Run 2028 was a DC-9 and 2034 was a B-727. On Day 118, Run 2006 was a B-727. Both runs on Day 115 produced tracks for only a single vortex, while on Day 118, two vortices were detected but there was a large amount of scatter in location. It should be noted that bad runs comprise less than 10% of all runs and less than 4% of those with large aircraft.

Evaluation of all three runs indicates that the spectra do not contain high amplitudes at high velocities. Run 2006 is especially interesting since the data from Van 1 indicates that the high velocity regions were in the scan area of both systems. Furthermore, in Runs 1004 and 2004, both vans produced good data on a B-727. The lack of high velocity components in the spectra indicates that the failure was not related to the processor, its settings, the software, or the parameters used in the algorithm. The only likely problem is that of alignment, although no notation was made in the log book concerning changes in alignment after any of these runs.

It is interesting to point out that although the spectral characteristics of these runs are very similar, the results are quite different. In the two runs on Day 115, the thresholds were sufficiently high to remove most of the data, leaving only a single vortex track. On Day 118, the spectrum was frequently above threshold, yielding several points for the processing algorithm. However, the choice of points to initiate the centroid algorithm was strongly influenced by noise. This is partly the result of the higher wind velocity on Day 118, which allowed more spectra to satisfy the velocity threshold.

These problems could probably be reduced by more careful monitoring of alignment of the laser and the optical system. In a more advanced system it might be possible to direct the scanner to a hard target between runs and allow the computer to recheck the range cali-

bration and SNR. In this way, degradations of the system due to alignment and other changes could be observed and corrected more quickly.

In summary, the system has been shown to be feasible for studying two phenomena with similar flow fields but very different backscatter coefficients and system requirements. Location accuracy of .2 range resolution elements is possible in real time, along with limited flow field information. In post analysis, a significant amount of flow field data is available which can be used to aid in the understanding of aircraft wake and naturally generated vortices.

## SECTION 6

## CONCLUSIONS

It has been shown that the Scanning Laser Doppler Velocimeter System is capable of detecting, locating, and tracking aircraft wake vortices in real time in an airport environment, and of detecting naturally occurring atmospheric vortices, such as dust devils. Over 1600 aircraft landings were monitored at Kennedy International Airport and near the end of the test period, over 95% of those runs involving larger aircraft produced usable results. Additionally, vortex flow field information has been obtained in a later analysis using the high speed tape data. Vortex velocity profiles, peak tangential velocities, and effective circulations have been calculated from this data. The real time location accuracy has been established at approximately 10 feet in range. This indicates that the vortex location algorithm is capable of locating an aircraft vortex to within approximately one-fifth of the system range resolution.

Approximately 80 dust devils were observed at the test site at Gila River Indian Reservation, south of Phoenix, Arizona and a number of these were analyzed in detail. The location accuracy was estimated to be approximately one-half the range resolution in these tests. The fact that the accuracy obtainable in location of aircraft wake vortices is not attainable for dust devils, is probably due to fluctuations in the backscatter coefficient of the dust devil. Thus, measurements of dust devils requiring accurate range location should be made with two systems and location determined by triangulation.

Also, in the dust devil measurements, a frequency translator was tested, and it was shown that the translator enables the system to determine the sense of the velocity. This is a substantial aid in analyzing complicated flow patterns, such as multiple vortices or multiple dust devils. The frequency translator made it possible to determine the direction of rotation of the dust devils and both

cyclonic and anti-cyclonic dust devils were observed.

In both the vortex and dust devil measurements, transport was generally shown to be as predicted theoretically and tracks were obtained within the anticipated range resolution accuracy.

The descent rates of aircraft vortices generally were measured to be considerably lower than those anticipated on the basis of a simple theory of wing tip vortices. Additionally, effective circulation measurements during the first fifteen seconds of a run were generally too high. These phenomena are probably associated with multiple vortices from the flaps, wing tips, and tail of the aircraft. Observations of vortex spectra indicate a more complicated spectral pattern in the early portion of a run. These facts suggest that at generation, the aircraft wake consists of a complicated multiple vortex pattern which, after approximately 10 to 15 seconds, rolls up into a single vortex pair.

A preliminary system re-design has been completed to design a smaller, more operational wake vortex detection system, and improved operating techniques have been established for optimizing the detection of both aircraft vortices and dust devils.

In summary, the Scanning Laser Doppler Velocimeter System has been shown to be an effective instrument for measuring aircraft wake vortices and naturally occurring atmospheric vortices, such as dust devils.